Theoretical and Experimental Studies on Thermal Behavior of 3-Methyl, 3-Carboxy, and 3-Nitro Substituted 1H,4H-6-nitro-pyrazolo[4,3-c]pyrazole

[1]Jiao-Qiang Zhang*, [2]Ning-Ning Zhao, [1]Hong-Yu Zhou, [2]Hai-Xia Ma, [3]Hong-Xu Gao
[3]Bo-Zhou Wang and [3]Rong-Zu Hu
[1]*Key Laboratory of Space Applied Physics and Chemistry of Ministry of Education, Department of Applied Chemistry, School of Science, Northwestern Polytechnical University, Xi'an 710129, China.*
[2]*College of Chemical Engineering/Shaanxi Key Laboratory of Physico-Inorganic Chemistry, Northwest University, Xi'an, 710069, China.*
[3]*Xi'an Modern Chemistry Institute, Xi'an, 710065, China*.
zhangjq@nwpu.edu.cn*

(Received on 15th February 2015, accepted in revised form 1st December 2016)

Summary: To evaluate the stability, heat-resistance ability and thermal safety of MNPP(1H,4H-3-methyl-6-nitro-pyrazolo[4,3-c]pyrazole), CNPP (1H,4H-3-carboxy-6 -nitro-pyrazolo[4,3-c]pyrazole), DNPP (1H,4H-3,6-dinitro-pyrazolo [4,3-c] pyrazole), the theoretical investigation on MNPP, CNPP and DNPP was performed by the DFT-B3LYP/6-31G level using Gaussian 09W program. The theoretical density (ρ) of the compounds was obtained by quantum chemical method. The Kamlet-Jacobs formulas were employed to calculate the detonation properties including the detonation velocity (D) and pressure (P). Their thermal behaviors were investigated by Differential Scanning Calorimetry (DSC), Thermogravimetry-Derivative Thermogravimetry (TG-DTG) and in-situ cell thermolysis/Rapid-Scan Fourier Transform Infrared Spectroscopy (RSFT-IR). Results show that (1) using critical temperature of thermal explosion, free energy of activation of decomposition reaction and self-accelerating decomposition temperature as criterions, the thermal stability, heat resistance ability and thermal safety of the three compounds decrease in the order of DNPP > MNPP >CNPP, but using energy gap and total energy as criterions, the thermal stability decreases in the order of DNPP > CNPP > MNPP, therefore, DNPP is the most stable compound among the three compounds; (2) Among of the three compounds, DNPP possesses the maximum theoretical density (1.80 g•cm^{-3}), the fastest detonation velocity (8.49 km•s^{-1}) and the highest detonation pressure (31.96 GPa), suggesting that DNPP has good detonation properties and potential use in energetic material.

Keywords: 1H,4H-3,6-dinitro-pyrazolo[4,3-c]pyrazole (DNPP), Theoretical calculation, Thermal behavior.

Introduction

High nitrogen heterocyclic compounds, as a series of promising energetic materials, possess the positive enthalpy of formation, high thermal stability and low sensitivity to impact and friction. In addition, it is worthy of noting that the high nitrogen content is also a key factor in increasing the density and obtaining good oxygen balance easily. Therefore, the high nitrogen heterocyclic compounds are widely used in solid propellants, explosives and civil combustible-gas generators [1, 4] as green energetic materials on the basis of their obvious advantages. It is reported that the density of DNPP (1H,4H-3,6-dinitro-pyrazolo[4,3-c]pyrazole) is 1.865 g•cm^{-3}, the nitrogen content is 42.42%, the heat of formation is 273 kJ•mol^{-1}, H_{50} is 68 cm and the energy tends to be 85% of octahydro-1,3,5,7-tetranitro- 1,3,5,7-tetrazocine (HMX) [5]. In addition, DNPP could be transferred to dinitropyrazolopyrazole anion (or dianion) and could be used to prepare DNPP amine salts [5, 6], which are particularly useful in gun propellant compositions. There is fused pyrazolopyrazole cycle in the DNPP molecular, in order to investigate how the different substituted groups on it will be influence the performances of the fused pyrazolopyrazole compounds, DNPP, MNPP (1H,4H-3-methyl-6-nitro-pyrazolo[4,3-c]pyrazole) and CNPP (1H,4H-3-carboxy-6-nitropyrazolo[4,3-c] pyra-zole) were designed and synthesized here, some theoretical calculations on these three compounds were carried out and the thermal behaviors of ones were also studied so as to find the potential application in energetic materials.

Experimental

Preparations of MNPP, CNPP and DNPP

All the three compounds (Fig. 1) were prepared according to the reference [6]. With acetylacetone and hydrazine hydrate as primary substance, MNPP was synthesized by the process of condensation, the first nitration, reduction, diazotization, intramolecular cyclic condensation and the second nitration in turn. M.p.263～265℃. Ana.

*To whom all correspondence should be addressed.

Calcd (%) for $C_5N_5H_5O_2$: C 35.94, N 41.91, H 3.02; found (%) C 35.87, N 41.77, H 2.99. IR (KBr) : 3431, 3247 (NH)，1505，1372 (NO_2)，1263, 1046, 1185 (CH, cyclo ring) cm^{-1}; ^{1}H-NMR (solv. acetone-d6, 400MHz) δ：2.43 (3H，CH_3), 12.25 (bs ,NH), 12.88 (bs, NH); ^{13}CNMR (solv. acetone-d6, 100MHz) δ： 11.51, 128.75，130.30, 136.77, 139.94. MNPP (0.4 g, 2.4 mmol) was dissolved in conc. H_2SO_4 (4.44 mL), $Na_2Cr_2O_7{\cdot}2H_2O$ (0.84 g, 2.83 mmol) was added over a period of 1 h at a temperature below 20 ℃, the mixture was agitated for 3 h at 20～30 ℃, the reaction mixture was poured into ice water (5×), and the precipitate was filtered, washed with ice-water, and dried in air, 0.4 g yellow CNPP powder was obtained, the yield was 84%. M.p. 263.7～265.5 ℃. IR (KBr) ν : 3596 (-OH), 3551, 3235 (NH)，1698 (C=O), 1506，1377 (NO_2)，1227, 1043, 1132(CH, cyclo ring) cm^{-1}; ^{1}H-NMR (solv. acetone-d6, 400MHz) δ： 13.50 (bs ，-NH);^{13}CNMR (solv. acetone-d6, 100MHz) δ：125.28, 131.08, 137.67, 139.44，161.92. DNPP was prepared as following: CNPP (3.5 g, 0.018 mol) was dissolved in pure nitric acid (50 mL), the mixture was stirred at 60 ℃. The reaction process was tracked and monitored by thin-layer chromatography. Then it was poured into ice water (5×), and the precipitate was filtered, washed with ice-water, and dried in air. The filtrate was extracted with ethyl acetate (3×20mL), the extracts were dried with $MgSO_4$, evaporated, and dried in vacuum oven, 2.7 g white DNPP powder was received, the yield was 77 %. The samples were purified by recrystallization with acetone for two times and kept in a vacuum drying oven before use. Ana. Calcd (%) for $C_4N_6H_2O_4$: C 24.42, N 42.42, H 1.01; found (%) C 24.37, N 42.17, H 1.18. IR (KBr) ν : 3267(NH)，1523，1373 (NO_2)，1245,1149,1039(cycle ring)cm^{-1}; ^{1}H-NMR (solv. acetone-d6, 400MHz) δ：13.60 (2H，-NH-); ^{13}CNMR (solv. acetone-d6, 100MHz) δ：139.24，132.65.

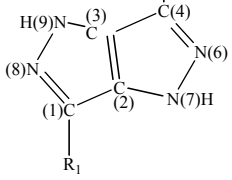

	R_1	R_2
MNPP	-N(10)O_2	-C(5)H_3
CNPP	-N(10)O_2	-C(5)OOH
DNPP	-N(10)O_2	-N(5)O_2

Fig. 1: The molecular structure of MNPP, CNPP and DNPP.

Quantum Chemical Investigation

Gaussian 09 [7] offers a wide variety of Density Functional Theory (DFT) models. B3LYP uses the non-local correlation provided by the LYP expression, and VWN functional III for local correlation (not functional V). Here, VWN: Vosko, Wilk, and Nusair 1980 correlation functional(III) fitting the random phase approximation（RPA） solution to the uniform electron gas, often referred to as Local Spin Density (LSD) correlation [8] (functional III in this article). LYP: The correlation functional of Lee, Yang, and Parr, which includes both local and non-local terms [9, 10].

The initial geometry of the three title compounds generated from Chem3D software was fully optimized at the DFT-B3LYP level by the Berny method [11, 12] with the 6-31G basis set. After that, the frequencies were calculated with the same method. There are no virtual frequencies, indicating that the optimized structures are in accord with the minimum points on the potential energy surfaces. All calculations were carried out on an IBM P4 computer with the Gaussian 09W program [7]. The accuracy of convergence took the default value of the program.

The theoretical density of the compounds was obtained from the molecular weight divided by the average molecular volume. The average mole volume of the compound was obtained from the statistical average value of 100 molar volumes. The mole volume of each molecule, defined as the volume inside a contour of 0.001 e/$bohr^3$ density [13] was calculated by the Monte Carlo method in the Gaussian 09W program package [7]. Qiu [14] has ever validated this method by comparing the experimental density with the calculated values for 45 energetic compounds. Most of these compounds are nitramines (N-NO_2-based), and the total average value of F_{cald}/F_{exptl} is more than 1.003.

The detonation velocity (*D*) and detonation pressure (*P*) were estimated by the Kamlet–Jacobs equation [15].

Thermal Decomposition Studies

The kinetic model function and kinetic parameters of the decomposition reaction of the three compounds were studied with Thermogravimetry-Derivative Thermogravimetry (TG-DTG) and Differential Scanning Calorimetry (DSC) using a model Q600SDT (TA, USA) in nitrogen atmosphere at a flow rate of 100 mL·min^{-1}. The heating rates used were 2.5, 5.0, 10.0 and 15.0 K•min^{-1} from ambient temperature to 700 K. The sample mass were about

0.0800 g. The temperature and heat were calibrated using pure indium and tin particles. The DSC and TG-DTG curves obtained under the same conditions overlap with each other, indicating that the reproducibility of tests is satisfactory.

In-Situ Cell thermolysis / Rapid-Scan Fourier Transform Infrared Spectroscopy (RSFT-IR) Analysis

In-situ cell thermolysis/RSFT-IR measurements were conducted using a model NEXUS 870 FT-IR spectrophotometer (Nicolet Instruments Co., USA) and in situ thermolysis cell (Xiamen University, P. R. China) with the temperature range of 20-455 ºC and heating rate of 10 ºC min^{-1}. KBr pellet samples, well mixed by about 0.7 mg DNPP and 150 mg KBr, were used. IR spectra of DNPP in the range1 of 4000-400 cm^{-1} were acquired by a model DTGS detector at a rate of 11 files min^{-1} and 8 scans file with a resolution of 4 cm^{-1}

Results and Discussion

The Optimized Structure

The main geometric parameters including the bond lengths, bond angles and dihedral angles of DNPP, CNPP, and MNPP are optimized and listed in Table-1. The results indicated that: (1) Almost all the ring atoms are in a same plane (the dihedrals are omitted in Table-1) form the conjugate π, the ring bonds tend to be equal. (2) The substitute groups of R_1 and R_2 seem to have little influence on the ring geometry of the compounds. (3) In MNPP, the longest bond is C-CH_3 (1.4930 Å) and in CNPP, the longest one is C-COOH (1.4554 Å), and in DNPP, the longest one is C-NO_2 (1.4282 Å), which shows these three bonds are the weakest in the three corresponding compounds and they are the trigger bonds in the compound. Furthermore, DNPP is the most stable one, then CNPP and MNPP does, when heated to some temperature.

The Stability of the Three Compounds

According to the molecular orbital (MO) theory, two important parameters, the highest occupied molecular orbital (HOMO) and the lowest unoccupied molecular orbital (LUMO), are investigated for studying the activities of compounds. The larger the energy gap $\triangle E$ (E_{LUMO}-E_{HOMO}) is, the more stable a compound will be. The results (Table-2) indicate that $\triangle E$ of DNPP is the largest among the three compounds, thus DNPP is the most stable compound among the three which is in accordance with the total energy result (the total energy of DNPP among the three compounds is the lowest), after DNPP is CNPP, then MNPP is the last in the list, which is consistent with the above molecular geometry results.

Table-1: Some selected calculated non-hydrogen bond lengths (in Å) and bond angles (in Deg) of MNPP, CNPP and DNPP

Bond length	MNPP	CNPP	DNPP
C(1)-C(2)	1.4127	1.4130	1.4133
C(1)-N(8)	1.3494	1.3483	1.3464
C(1)-N(10)	1.4240	1.4262	1.4281
C(2)-C(3)	1.4011	1.3972	1.3983
C(2)-N(7)	1.3590	1.3673	1.3692
C(3)-C(4)	1.4276	1.4212	1.4133
C(3)-N(9)	1.3812	1.3714	1.3692
C(4)-C(5)	1.4930	1.4554	
C(4)-N(5)			1.4282
C(4)-N(6)	1.3505	1.3552	1.3464
N(6)-N(7)	1.3902	1.3728	1.3684
N(8)-N(9)	1.3666	1.3680	1.3684
Bond angle			
A(C2,C1,N8)	111.17	111.02	110.96
A(C2,C1,N10)	126.06	125.88	125.71
A(N8,C1,N10)	122.77	123.10	123.33
A(C1,C2,C3)	105.67	105.35	105.22
A(C1,C2,N7)	147.67	148.28	148.13
A(C3,C2,N7)	106.66	106.37	106.65
A(C2,C3,C4)	106.99	106.41	105.22
A(C2,C3,N9)	105.77	106.46	106.65
A(C4,C3,N9)	147.24	147.12	148.13
A(C3,C4,C5)	130.62	125.01	125.71
A(C3,C4,N6)	108.29	109.31	110.96
A(C5,C4,N6)	121.10	125.68	123.33
A(C4,N6,N7)	107.38	106.42	105.59
A(C2,N7,N6)	110.68	111.50	111.58
A(C1,N8,N9)	105.24	105.38	105.59
A(C3,N9,N8)	112.16	111.79	111.58

Table-2: Total Energies (E_{total}) and energy gap (ΔE_{L-H}) of the three compounds (in hartree).

	E_{HOMO}	E_{LUMO}	ΔE_{L-H}	E_{total}
MNPP	-0.26279	-0.11022	0.15257	-617.36805
CNPP	-0.28798	-0.12323	0.16475	-766.55820
DNPP	-0.30916	-0.14298	0.16618	-782.33989

Detonation Properties

The values of detonation velocity (D) and pressure (P) play a key role in evaluating the detonation performances of the explosives. The values of the two important targets can be obtained by the Kamlet–Jacobs formulae shown as the following equations (1)-(3) [16].

$$D = 1.01 \times \Phi^{0.5}(1.0 + 1.3\rho) \quad (1)$$

$$\Phi = N\bar{M}^{0.5}Q^{0.5} \quad (2)$$

$$P = 1.558 \times \Phi\rho^2 \quad (3)$$

where D is the detonation velocity (km•s^{-1}), Φ is the characteristics value of explosives, ρ is the packed density (g•cm^{-3}, Table-3), P is the detonation pressure (GPa), N is the moles of gas produced by per gram of

explosives, $\bar{M}$ is an average molar weight of detonation products, and Q is the chemical energy of detonation (kJ•g^{-1})

Table-3: The average molar volume (V), heats of formation at 298K ($\Delta_f H^{\theta}_{298}$), theoretical densities (ρ), the detonation velocity (D) and pressure (P) of MNPP, CNPP and DNPP.

Compound	V/(cm^3• mol^{-1})	$\Delta_f H^{\theta}_{298}$/(k J•mol^{-1})	ρ/(g•c m^{-3})	D/(km •s^{-1})	P/G Pa
MNPP $C_5N_5H_5O_2$	108.19	528.19	1.54	7.61	23.25
CNPP $C_5N_5H_3O_4$	115.69	222.50	1.70	7.38	23.32
DNPP $C_4N_6H_2O_4$	109.75	577.85	1.80	8.49	31.96

Based on the calculated results at DFT-B3LYP/6-31G method, the heat of formations (HOFs) of the three compounds at 298 K were carried out using the equation (5) from the atomization reaction (4).

$$C_aH_bN_cO_d \rightarrow aC(g)+bH(g)+cN(g)+dO(g) \qquad (4)$$

For the atomization reaction (4), heat of reaction $\Delta_f H^{\theta}_{298}$ at 298 K can be calculated by equation (5):

$$\Delta_f H^{\theta}_{298} = \sum \Delta_f H^{\theta}_{298,P} - \sum \Delta_f H^{\theta}_{298,R}$$

$$= a\Delta_f H^{\theta}_{298,C} + b\Delta_f H^{\theta}_{298,H} + c\Delta_f H^{\theta}_{298,N} + d\Delta_f H^{\theta}_{298,O} - \Delta_f H^{\theta}_{298,CaHbNcOd} \qquad (5)$$

where $\sum \Delta_f H^{\theta}_{298,p}$ and $\sum \Delta_f H^{\theta}_{298,R}$ are sums of the HOFs for products and reactants in gas at 298 K, respectively. $\Delta_f H^{\theta}_{298,C}$, $\Delta_f H^{\theta}_{298,H}$, $\Delta_f H^{\theta}_{298,N}$ and $\Delta_f H^{\theta}_{298,O}$ are the HOFs of C, H, N and O atoms at 298 K as seen in Table-4, respectively. Either the both of G2 theory [17] or the complete basis set (CBS-Q) method [18, 19] can be able to obtain the HOFs accurately, whereas the G2 theory is more expensive and not yet practical to calculate the total energies of these aza cyclic skeletons due to the large ring size. Therefore, the CBS-Q method was used in this work. The ΔH^{θ}_{298} can be calculated using the following expression:

$$\Delta_f H^{\theta}_{298} = \Delta E_{298} + \Delta(pV) \qquad (6)$$

$$\Delta E_{298} = \Delta E_0 + \Delta E_{ZPE} + \Delta(H^0_{298} - H^0_0) \qquad (7)$$

$$\Delta(pV) = \Delta nRT = (a+b+c+d-1)RT \qquad (8)$$

where ΔE_0 is the change in total energy between the products and the reactants at 0 K; ΔE_{ZPE} is the difference between the zero-point energies (ZPE) of the products and the reactants at 0 K; $\Delta(H^0_{298} - H^0_0)$ is thermal correction from 0 to 298 K. The $\Delta(pV)$ value in Eqs. (6) and (8) is the PV work term and equals ΔnRT for the reactions of ideal gas. For the atoms here, E_{ZPE} = 0, $H^0_{298} - H^0_0$ = 0. So

$$\Delta E_{298} = aE_{0,C} + bE_{0,H} + cE_{0,N} + dE_{0,O} - E_{0,CaHbNcOd} - E_{ZPE,CaHbNcOd} - \Delta H^{\theta}_{T,CaHbNcOd} \qquad (9)$$

where $E_{0,C}$, $E_{0,H}$, $E_{0,N}$, $E_{0,O}$ and $E_{0,CaHbNcOd}$ are the total energies of C, H, N, O atoms and $C_aH_bN_cO_d$ at DFT-B3LYP/6-31G method respectively. $E_{ZPE,CaHbNcOd}$ and $\Delta H^{\theta}_{T,CaHbNcOd}$ are the zero-point correction energy and the thermal correction to Enthalpy of $C_aH_bN_cO_d$ respectively. ΔH^{θ}_{298} can be calculated from Eqs. (5) – (9). The $\Delta_f H^{\theta}_{298}$ values of MNPP, CNPP and DNPP are 528.19, 222.50 and 577.85 kJ•mol^{-1}, respectively. Therefore, the values of Q (Eq. 2) could be obtained. The Q values of MNPP, CNPP and DNPP are 1.45, 1.31 and 1.70 kJ•g^{-1}, respectively. Based on the ρ and Q values, the related D and P values of MNPP, CNPP and DNPP were listed in Table-3. The ρ, D and P values of DNPP are the largest among the three compounds, therefore it has the potential use in explosives, further we carried the thermal behavior researches on these three compounds.

Table-4: Experimental heats of formation and calculated total energies for C, H, N and O atoms.

	$\Delta_f H^{\theta}_{atom}$ / (kJ•mol^{-1})	E_0/a.u. at B3LYP/6-31G level (Hartree)
C	716.7	-37.84366
H	218.0	-0.50027
N	472.7	-54.58287
O	249.2	-75.05833

Thermal Behavior

As the Figs. 2 and 3 show, the DSC, TG-DTG data are obtained at a heating rate of 10 K•min^{-1}. From the DSC curve in Fig. 2, it can be found that only one exothermic change with the peak maximum at 601.76 K during the total thermal decomposition process of DNPP, corresponding to the one stage of a quick mass loss shown in the TG-DTG curve in Fig. 3. The quick mass loss of 68.53% occurred in the temperature ranges 588.19~658.93 K with the peak temperature of 599.54 K.

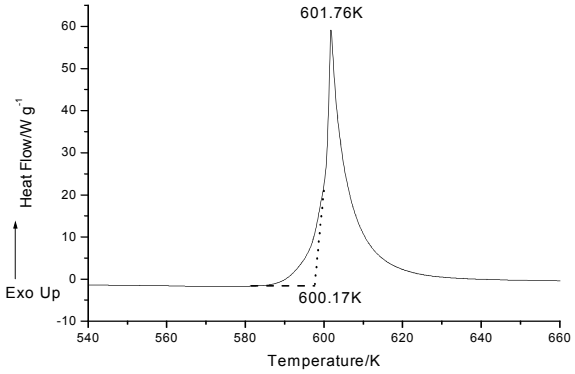

Fig. 2: DSC curve of DNPP at heating rate of 10 K•min$^{-1.}$

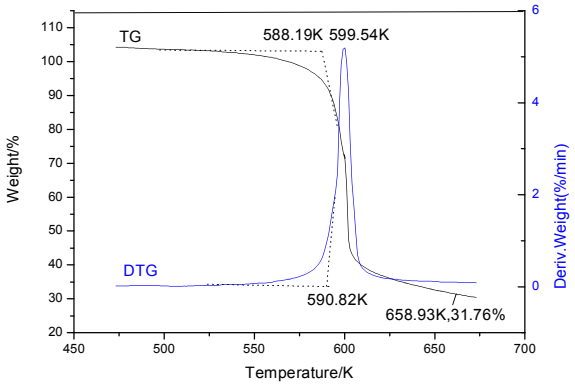

Fig. 3: TG-DTG curve of DNPP at heating rate of 10 K•min$^{-1.}$

Non-Isothermal Kinetics Parameters Based on Peak Temperature and Onset Temperature at Different Heating Rates

Two model-free isoconversional methods shown as Eqs. (10) and (11) were used to calculate the apparent activation energy (E_a) and pre-exponential factor (A) for evaluating the exothermic decomposition processes of the three title compounds. These methods are as follows:

Differential method

Kissinger equation [20]

$$\frac{\mathrm{d}\ln\frac{\beta}{T_p^2}}{\mathrm{d}\frac{1}{T_p}} = -\frac{E_\alpha}{R} \qquad (10)$$

Integral method

Flynn-Wall-Ozawa (F-W-O) equation [21, 22]

$$\lg\beta + \frac{0.4567\,E_\alpha}{RT} = C \qquad (11)$$

where α is the conversion degree, T is the absolute temperature, E_α is the apparent activation energy, β is the heating rate, R is the gas constant, T_p is the peak temperature of DSC curve, A is the pre-exponential factor.

From Table-5 and 6, E_α obtained with T_{pi} versus β_i relation by the Kissinger [20] method is determined to be 320.83 kJ•mol^{-1} for DNPP, 278.44 kJ•mol^{-1} for MNPP and 100.05 kJ•mol^{-1} for CNPP. The pre-exponential constant (A) is $10^{26.11}$ s^{-1} for DNPP, and $10^{23.54}$ s^{-1} for MNPP and $10^{6.83}$ s^{-1} for CNPP. The linear correlation coefficient (r_k) is 0.9940 for DNPP, 0.9965 for MNPP and 0.9556 for CNPP. The value of E_α obtained with T_{pi} versus β_i relation by Ozawa's method [21] is 314.52 kJ•mol^{-1} for DNPP, 273.80 kJ•mol^{-1} for MNPP and 104.09 kJ•mol^{-1} for CNPP, the value of r_o is 0.9943 for DNPP, 0.9968 for MNPP and 0.9865 for CNPP. The E_{oe} values of DNPP, MNPP and CNPP are 264.31, 389.44. and 109.38 kJ•mol^{-1}, respectively, which are obtained by T_{ei} versus β_i relations. The value of r_{oe} is 0.9919 for DNPP, 0.9958 for MNPP and 0.9556 for CNPP. E_o obtained by T_{ei} and T_{pi} have a deviation of 50.21 kJ•mol^{-1}for DNPP and -95.64 kJ•mol^{-1}for MNPP and -5.29 kJ•mol^{-1}for CNPP.

Table-5: Values of the kinetic parameters for the exothermic decomposition reaction for the three compounds calculated from the DSC curves at various heating rates and a flowing rate of N_2 gas of 100 mL•min^{-1}

β/(℃•min^{-1})	T_e/℃			T_p/℃		
	DNPP	CNPP	MNPP	DNPP	CNPP	MNPP
2.5	310.93	265.56	284.28	315.47	272.57	289.05
5.0	318.74	270.46	288.98	323.03	284.60	294.06
10.0	327.01	295.90	293.89	328.61	308.17	301.49
15.0	328.82	297.80	295.42	331.35	312.04	305.53

[a]β, heating rate ; T_e, onset temperature in the DSC curve; T_p, maximum peak temperature.

From Fig. 1 and Table-5, replacing R_2=-CH_3 in MNPP and R_2=-COOH in CNPP with R_2=-NO_2 increases the thermal stability, showing that the symmetry of the molecular structure is a principal faction affecting the thermal stability.

Mechanism of Thermal Decomposition

By substituting the original data β_i, T_{0i}, T_i, and α_i, i=1, 2, n, tabulated in Table7 from DSC curve of DNPP into Eq. (11), the values of E_α for any given value of α in Table-6 are obtained (Fig. 4), the results obtained from the TG curves of DNPP and MNPP are showed in Fig. 5.

Table-6: The kinetic data of DNPP, CNPP and MNPP calculated from the DSC curves at four heating rates.

	E_{oe}/ (kJ•mol^{-1})	r_{oe}	E_k/ (kJ•mol^{-1})	lg(A_k/s^{-1})	r_k	E_o/ (kJ•mol^{-1})	r_o
DNPP	**264.31**	**0.9919**	**320.83**	**26.11**	**0.9940**	**314.52**	**0.9943**
CNPP	**109.38**	**0.9556**	**100.05**	**6.83**	**0.9838**	**104.09**	**0.9865**
MNPP	**389.44**	**0.9958**	**278.44**	**23.54**	**0.9965**	**273.80**	**0.9968**

[a]*E*, apparent activation energy; *A*, pre-exponential constant; *r*, linear correlation coefficient; subscript *k*, data obtained by Kissinger's method, subscript o, data obtained by Ozawa's method. E_{oe} means the activation energy obtained by T_e through Ozawa's method and r_{oe} is the corresponding linear correlation coefficient.

Table-7: Data of DNPP determined by DSC at different heating rates and apparent activation energies (E_a) of thermal decomposition obtained using isoconversional methods

Data Point	α	$T_{2.5}$/K	T_5/K	T_{10}/K	T_{15}/K	E_α/(kJ•mol^{-1})
1	**0.025**	**581.26**	**589.74**	**597.70**	**599.25**	**259.51**
2	**0.050**	**582.11**	**590.81**	**599.76**	**603.02**	**231.73**
3	**0.075**	**582.85**	**591.66**	**601.09**	**603.75**	**229.14**
4	**0.100**	**583.51**	**592.38**	**601.42**	**604.10**	**233.81**
5	**0.125**	**584.10**	**593.00**	**601.60**	**604.35**	**239.18**
6	**0.150**	**584.63**	**593.55**	**601.73**	**604.56**	**244.44**
7	**0.175**	**585.11**	**594.06**	**601.85**	**604.77**	**249.19**
8	**0.200**	**585.55**	**594.53**	**601.97**	**604.98**	**253.43**
9	**0.225**	**585.95**	**594.97**	**602.1**	**605.20**	**256.99**
10	**0.250**	**586.31**	**595.35**	**602.24**	**605.43**	**259.80**
11	**0.275**	**586.65**	**595.67**	**602.39**	**605.68**	**262.03**
12	**0.300**	**586.96**	**595.91**	**602.54**	**605.95**	**263.58**
13	**0.325**	**587.25**	**596.10**	**602.72**	**606.23**	**264.50**
14	**0.350**	**587.51**	**596.26**	**602.90**	**606.53**	**264.73**
15	**0.375**	**587.76**	**596.40**	**603.10**	**606.85**	**264.44**
16	**0.400**	**587.99**	**596.53**	**603.31**	**607.19**	**263.57**
17	**0.425**	**588.20**	**596.66**	**603.54**	**607.56**	**261.98**
18	**0.450**	**588.40**	**596.80**	**603.78**	**607.94**	**260.10**
19	**0.475**	**588.57**	**596.94**	**604.04**	**608.35**	**257.43**
20	**0.500**	**588.74**	**597.10**	**604.32**	**608.80**	**254.37**
21	**0.525**	**588.89**	**597.25**	**604.62**	**609.27**	**250.79**
22	**0.550**	**589.03**	**597.43**	**604.95**	**609.78**	**246.76**
23	**0.575**	**589.19**	**597.62**	**605.30**	**610.33**	**242.65**
24	**0.600**	**589.35**	**597.83**	**605.69**	**610.93**	**238.13**
25	**0.625**	**589.52**	**598.06**	**606.11**	**611.58**	**233.38**
26	**0.650**	**589.70**	**598.33**	**606.57**	**612.29**	**228.38**
27	**0.675**	**589.91**	**598.62**	**607.08**	**613.08**	**223.13**
28	**0.700**	**590.14**	**598.95**	**607.66**	**613.96**	**217.50**
29	**0.725**	**590.41**	**599.34**	**608.30**	**614.95**	**211.66**
30	**0.750**	**590.73**	**599.80**	**609.03**	**616.06**	**205.63**
31	**0.775**	**591.11**	**600.35**	**609.88**	**617.35**	**199.14**
32	**0.800**	**591.58**	**601.03**	**610.88**	**618.85**	**192.34**
33	**0.825**	**592.19**	**601.91**	**612.09**	**620.63**	**185.30**
34	**0.850**	**593.00**	**603.06**	**613.60**	**622.8**	**177.87**
35	**0.875**	**594.14**	**604.66**	**615.54**	**625.52**	**170.25**
36	**0.900**	**595.84**	**607.02**	**618.17**	**629.07**	**162.58**
37	**0.925**	**598.52**	**610.80**	**622.01**	**633.97**	**155.03**
38	**0.950**	**603.21**	**617.06**	**628.36**	**641.25**	**147.98**
39	**0.975**	**612.76**	**628.22**	**640.47**	**653.37**	**143.39**
40	**1.000**	**648.03**	**654.34**	**658.96**	**668.03**	**311.93**

T with the subscript 2.5, 5.0, 10.0, 15.0 are the temperature obtained at the heating rates of 2.5, 5.0, 10.0, 15.0 °C•min^{-1} respectively. *E* with the subscript F-W-O is the activation energy calculated by F-W-O eqs.

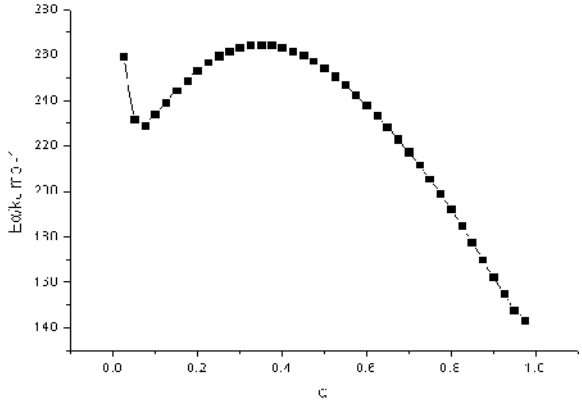

Fig. 4: E_a vs α curve of DNPP by Flynn-Wall-Ozawa's method.(The title of Y-axis is E_a not E_α.)

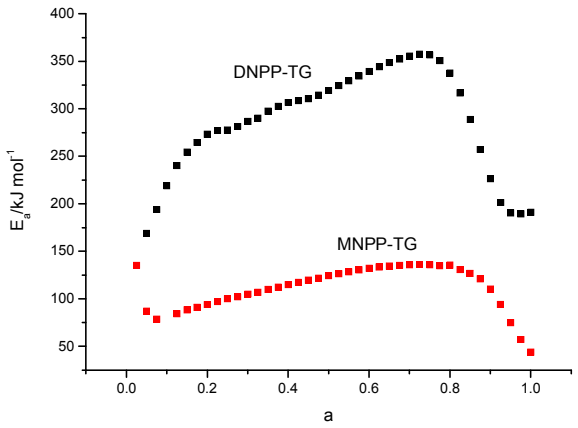

Fig. 5: E_a vs α curves obtained from the TG data of DNPP and MNPP by Flynn-Wall-Ozawa's method.

From Fig. 4 and 5, one can see that the values of E_a vary in the α range of 0~1.00, indicating that each thermal decomposition process of DNPP, MNPP and CNPP is a multiple reaction. Therefore, it is difficult to properly interpret the kinetics and mechanism of the thermal decomposition depending on the relationship between the E_a and α.

Self-Accelerating Decomposition Temperature (T_{eo} and T_{po})

The values (T_{eo} and T_{po}) of the onset temperature (T_e) and T_p corresponding to $\beta \rightarrow 0$ obtained by Eq. (12) taken from [23] are 302.05 °C and 304.73 °C for DNPP, 279.16 °C, 283.20 °C for MNPP, 247.58 °C and 252.53 °C for CNPP indicating that the heat-resistance abilities of DNPP, MNPP and CNPP decrease in the order of DNPP > MNPP > CNPP. This shows that DNPP has better heat-resistance.

$$T_{e\ or\ p} = T_{eo\ or\ po} + a\beta_i + b\beta_i^2 \quad i=1\sim4 \qquad (12)$$

where *a* and *b* are coefficients.

Critical Temperature of Thermal Explosion (T_{be} and T_{bp})

The corresponding critical temperatures of thermal explosion (T_b) obtained from Eq. (13) taken from [24] is 312.85 (T_{be}) and 313.83 °C (T_{bp}) for

DNPP and 285.83 (T_{be}) and 292.93 °C (T_{bp}) for MNPP, 271.25 °C (T_{be}) and 276.68 °C (T_{bp}) for CNPP, showing that the transition resistance from thermal decomposition to thermal explosion decreases in the order of DNPP > MNPP >CNPP. This shows that DNPP has better thermal safety.

$$T_b = \frac{E_{oe,or,op} - \sqrt{E_{oe,or,op}^2 - 4E_{oe,or,op}RT_{e0,or,p0}}}{2R} \quad (13)$$

where R is the gas constant (8.314 J•mol^{-1}•K^{-1}), E_o is the value of E obtained by Ozawa's method.

Calculation of $\Delta S^{\neq}$, $\Delta H^{\neq}$and $\Delta G^{\neq}$

The entropy of activation ($\Delta S^{\neq}$) corresponding to $T = T_{pdo}$, $E_a = E_k$ and $A = A_k$ obtained by Eqs. (14), (15) and (16) are 241.22, 192.23 and -127.19 J•mol^{-1}•K^{-1} for DNPP, MNPP and CNPP, respectively. The enthalpy of activation ($\Delta H^{\neq}$) corresponding to $T = T_{pdo}$, $E_a = E_k$ and $A = A_k$ obtained by Eqs. (14), (15) and (16) are 316.08, 273.81 and 95.68 kJ•mol^{-1} for DNPP, MNPP and CNPP, respectively. The free energy of activation ($\Delta G^{\neq}$) corresponding to $T = T_{pdo}$, $E_a = E_k$ and $A = A_k$ obtained by Eqs. (14), (15) and (16) are 178.38, 166.87 and 162.54 kJ•mol^{-1} for DNPP, MNPP and CNPP, respectively. The results reveal that the relation thermal stability decreases in the order of DNPP > MNPP > CNPP.

$$A = \frac{k_B T}{h} e^{\Delta S^{\neq}/R} \quad (14)$$

$$\Delta H^{\neq} = E_a - RT \quad (15)$$

$$\Delta G^{\neq} = \Delta H^{\neq} - T\Delta S^{\neq} \quad (16)$$

where k_B is the Boltzmann constant, h is the Plank constant.

In-Situ cell Thermolysis/RSFT-IR Analysis

In-situ cell thermolysis/RSFT-IR was employed to analyze the condensed phase products of the thermal decomposition of DNPP under the linear temperature rise conditions in real-time. Fig. 6 shows the RSFT-IR spectrum of DNPP at room temperature (20 ºC). The ν_{as} C-NO_2 and ν_s C-NO_2 peaks at 1523 cm^{-1} and 1345 (or 1349) cm^{-1}, δ_{C-NO_2} peaks at 839 cm^{-1} and δ_{-NO_2} peak at 656 cm^{-1} for the C-NO_2 bonds, the ν_{N-H} peak at 3268 cm^{-1} and the ν_{C-N} peak of secondary amine (bending vibrations) at 1370 cm^{-1}, δ_{N-H} peaks at 1548 cm^{-1} for the N-H bonds, δ_{C-H} peak at 1430 cm^{-1} (bending vibrations), δ-ring peaks at 1245, 1149 and 1039 cm^{-1} *et. al.* can be observed.

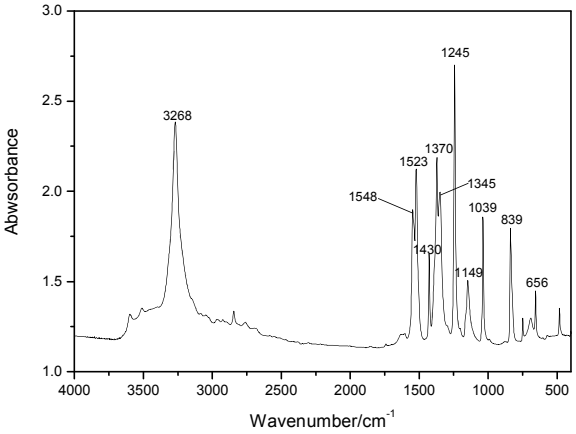

Fig. 6: The in-situ cell thermolysis/RSFT-IR spectrum of DNPP at room temperature (20 ℃).

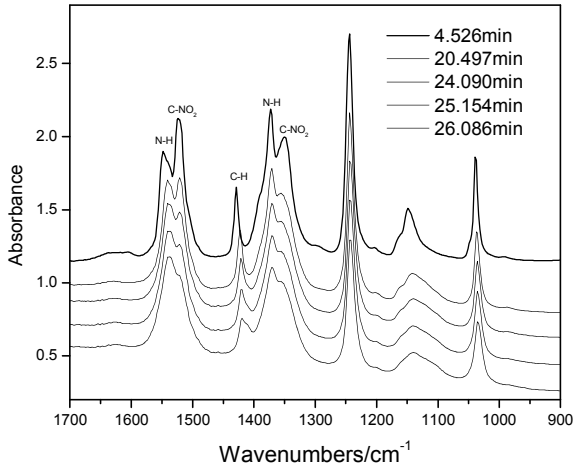

Fig. 7: In-situ cell thermolysis/RSFT-IR spectra of the condensed phase of DNPP at different time (temperatures).

The IR spectra of the condensed phase products of DNPP at different temperatures are shown in Fig.7. It can be found that the comparatively intensity of the ν_{as} C-NO_2 peak at 1523 and 1345 cm^{-1} weakens earlier more than the δ_{N-H} peak at 1548 cm^{-1} and ν_{C-N} peak of secondary amine at 1370 cm^{-1}, which mean that the NO_2 is the first removed group when

DNPP was heated to 250 ℃, and then the fused pyrazolopyrazole cycle is opened, which is accordant with the above theoretical calculations. When the NO_2 group is broken away from the DNPP molecular structure, the chemical atmosphere of C-H bond is changed, which induce the variety of vibration frequency of the C-H bonds, this will be embodied as shifts of the characteristic absorption bands, in Fig.6, δ_{C-H} peak at 1430 cm^{-1}(bending vibrations) is transferred to 1423 cm^{-1} and then 1420 cm^{-1} *et. al.* as the temperature going on.

Conclusion

1. Using $\triangle E=E_{LUMO}-E_{HOMO}$ and E_{total} as criterions, the stability of DNPP, MNPP and CNPP decreases in the order of DNPP > CNPP > MNPP, DNPP is the most stable compound among DNPP, CNPP and MNPP.
2. Using T_{eo}, T_{po}, T_{be}, T_{bp} as criterions, the heat resistance abilities and the transition resistance during the thermal decomposition process of DNPP, MNPP and CNPP decrease in the order of DNPP > MNPP > CNPP, showing that DNPP has better thermal safety and heat-resistance ability.
3. The whole thermal decompositions of DNPP and MNPP cannot follow one fixed mechanism.
4. Using $\Delta G^{\neq}$ as criterion, the relative thermal stability of DNPP, MNPP and CNPP decreases in the order DNPP > MNPP > CNPP.
5. The calculated density, detonation velocity and detonation pressure of DNPP are 1.80 $g•cm^{-3}$, 8.49 $km•s^{-1}$ and 31.96 GPa, respectively. It can be used as a potential energetic material.

Acknowledgements

This work was supported by the National Natural Science Foundation of China (No. 21673182), Program for New Century Excellent Talents in University of Ministry of Education of China (NCET-12-1047).

References

1. D. M. Badgujar, M. B.Talawar, S. N. Asthana and P. P. Mahulikar, Advances in Science and Technology of Modern Energetic Materials: An Overview, *J. Hazard. Mater.,* **151**, 289 (2008).
2. P. F. Pagoria, G. S. Lee, A. R. Mitchell and R. D. Schmidt, A Review of Energetic Materials Synthesis, Thermochim. Acta, **384**, 187 (2002).
3. N. Saracoglu, Recent Advances and Applications in 1,2,4,5-Tetrazine Chemistry, *Tetrahedron,* **63**, 4199 (2007).
4. M. B. Talawar, R. Sivabalan, T. Mukundan, H. Muthurajan, A. K. Sikder, B. R. Gandhe, and A. S. Rao, Environmentally Compatible Next Generation Green Energetic Materials (GEMs), *J. Hazard. Mater*, **161**, 589 (2009).
5. A. G. Stern, J. S. Moran, R. J. Jouet, M. E. Sitzman, P. F. Pagoria and G. S. Lee, Dinitropyrazolopyrazole-amine Salts Useful in Gun Propellants, Patent-US 6706889 (2004).
6. Y. F. Luo, Z. X. Ge, B. Z. Wang, H. H. Zhang and Q. Liu, Synthetic Improvement of DNPP, *Chin. J. Energ. Mater.*, **15**, 205 (2007).
7. M. J. Frisch, G. W. Trucks, H. B. Schlegel, G. E.Scuseria, M. A. Robb, J. R. Cheeseman, G. Scalmani, V. Barone, B. Mennucci, G. A. Petersson, H. Nakatsuji, M. Caricato, X. Li, H. P. Hratchian, A. F. Izmaylov, J. Bloino, G. Zheng, J. L. Sonnenberg, M. Hada, M. Ehara, K. Toyota, R. Fukuda, J. Hasegawa, M. Ishida, T. Nakajima, Y. Honda, O. Kitao, H. Nakai, T. Vreven, J. A. Montgomery, Jr. J. E. Peralta, F. Ogliaro, M. Bearpark, J. J. Heyd, E. Brothers, K. N. Kudin, V. N. Staroverov, R. Kobayashi, J. Normand, K. Raghavachari, A. Rendell, J. C. Burant, S. S. Iyengar, J. Tomasi, M. Cossi, N. Rega, J. M. Millam, M. Klene, J. E. Knox, J. B. Cross, V. Bakken, C. Adamo, J. Jaramillo, R. Gomperts, R. E. Stratmann, O.Yazyev, A. J. Austin, R. Cammi, C. Pomelli, J. W. Ochterski, R. L. Martin, K. Morokuma, V. G. Zakrzewski, G. A.Voth, P. Salvador, J. J. Dannenberg, S. Dapprich, A. D. Daniels, Ö. Farkas, J. B. Foresman, J. V. Ortiz, J. Cioslowski and D. J. Fox, *Gaussian 09*, Revision A.02. Wallingford, CT: 2009. Gaussian, Inc.
8. S. H. Vosko, L. Wilk and M. Nusair, Accurate Spin-Dependent Electron Liquid Correlation Energies for Local Spin Density Calculations: A Critical Analysis, *Can. J. Phys.,* **58**, 1200 (1980).
9. C. Lee, W. Yang, R. G. Parr, Development of the Colle-Salvetti Correlation-Energy Formula into a Functional of the Electron Density, *Phys. Rev.* B., **37**, 785 (1988).
10. B. Miehlich, A. Savin, H. Stoll and H. Preuss, Results Obtained with the Correlation-Energy Density Functionals of Becke and Lee, Yang and Parr, *Chem. Phys. Lett.,* **157**, 200 (1989).
11. R. Fletcher, and M. J. D. Powell, A Rapidly Convergent Descent Method for Minimization, *Comput. J.,* **6**, 163 (1963).
12. H. B. Schlegel, Optimization of Equilibrium Geometries and Transition Structures, *J. Comput.*

Chem., 3, 214 (1982).

13. M. W. Wong, K. B. Wiberg and M. J. *J.* Frisch, Ab Initio Calculation of Molar Volumes: Comparison with Experiment and Use in Solvation Models, *Comput. Chem.,* **16**, 385 (1995).
14. L. Qiu, H. M. Xiao, X. D. Gong, X. H. Ju and W. H. Zhu, Crystal Density Predictions for Nitramines Based on Quantum Chemistry, *J. Hazard. Mater.*, **141**, 280 (2007).
15. M. J. Kamlet and S. J. Jacobs, A Simple Method for Calculating Detonation Properties of C-H-N-O Explosives, *J. Chem. Phys.,* **48**, 23 (1968).
16. X. H. Zhang and Z. H. Yun, Explosive Chemistry, National Defense Industry Press, Beijing, (1989).
17. L. A. Curtiss, K. Raghavachari, P. C. Redfern and J. A. Pople, Assessment of Gaussian-2 and Density Functional Theories for the Computation of Enthalpies of Formation, *J. Chem. Phys*., **106**, 1063 (1997).
18. J. W. Ochterski, G. A. Petersson, J. A. Montgomery, A Complete Basis Set Model Chemistry.5. Extensions to Six or More Heavy Atoms, J. Chem. Phys., 104, 2598 (1996).
19. B. S. Jursic, Computing the Heat of Formation for Cubane and Tetrahedrane with Density Functional Theory and Complete Basis Set ab Initio Methods, J. Mol. Struct.: THEOCHEM, 499, 137 (2000).
20. H. E. Kissinger, Reaction Kinetics in Differential Thermal Analysis, Anal. Chem., 29, 1702 (1957).
21. T. Ozawa, A New Method of Analyzing Thermogravimetric Data, *Bull. Chem. Soc. Jpn.,* **38**, 1881 (1965).
22. J. H. Flynn and L. A. Wall, A Quick, Direct Method for the Determination of Activation Energy from Thermogravimetric Data, *J. Polym. Sci., Part B: Polym. Lett.,* **4**, 325 (1966).
23. R. Z. Hu, Z. Q. Yang and Y. J. Liang, The Determination of the Most Probable Mechanism Function and 3 Kinetic-Parameters of Exothermic Decomposition Reaction of Energetic Materials by a Single Non-Isothermal DSC Curve, *Thermochim. Acta*, **123**, 135 (1988).
24. R. Z. Hu and Q. Z. Shi, Thermal Analysis Kinetics, Science Press, Beijing, p.127 (2001) (in Chinese).